Institute of Paper Science and Technology
Atlanta, Georgia

IPST TECHNICAL PAPER SERIES

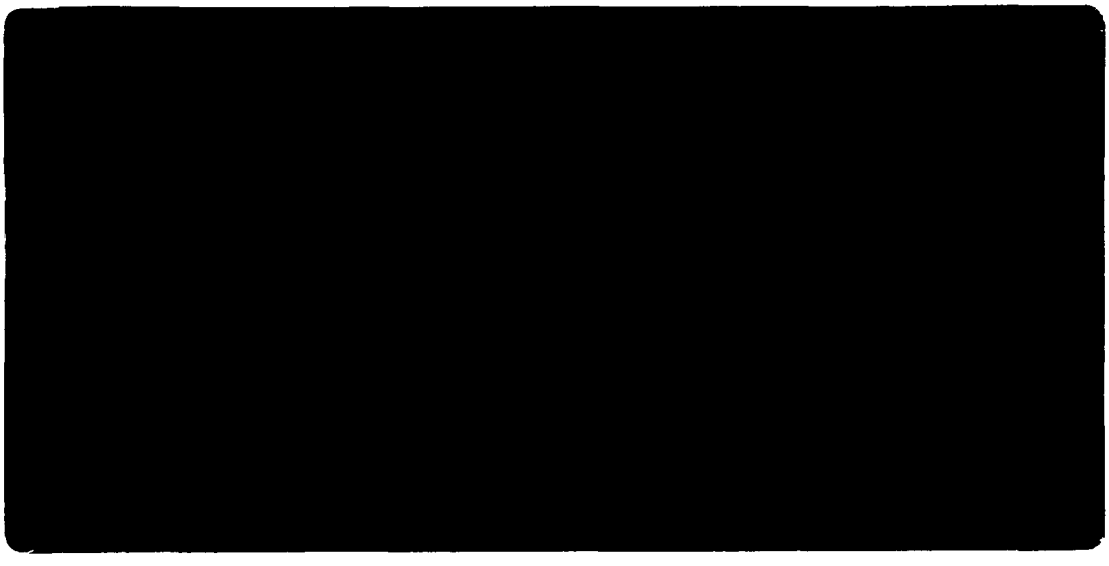

NUMBER 442

CO_2 GASIFICATION OF KRAFT BLACK LIQUOR CHAR IN A FIXED BED REACTOR

S.R. LEE AND K.M. NICHOLS

MAY 1992

CO_2 Gasification of Kraft Black Liquor Char in a Fixed Bed Reactor

S.R. Lee and K.M. Nichols

Submitted to
Journal of Pulp and Paper Science

CO_2 GASIFICATION OF KRAFT BLACK LIQUOR CHAR IN A FIXED BED REACTOR

STACY R. LEE AND KENNETH M. NICHOLS
GRADUATE STUDENT AND ASSISTANT PROFESSOR OF ENGINEERING
INSTITUTE OF PAPER SCIENCE & TECHNOLOGY
575 14th STREET, N.W.
ATLANTA, GA 30318

For Submission to the Journal of Pulp and Paper Science, April 7, 1992

ABSTRACT

The CO_2 gasification rate of kraft black liquor char was studied using a fixed bed reactor at temperatures of 600°C, 700°C, and 800°C. The rate and the activation energy (E_A = 48 kcal/mol) compare well to rates and activation energies reported previously from thermogravimetric measurements of kraft char gasification. Mass transfer limitations on the observed rate were determined to be negligible by changing both carrier gas and flow rates. Application of the rate derived from the fixed bed reactor to a recovery furnace char bed at typical operating conditions predicts that the rate of CO_2 gasification on the bed is mass transfer controlled at temperatures of 800°C or greater.

INTRODUCTION

Strong black liquor burns in air in three stages known as drying, devolatilization, and char burning [1,2]. Drying involves the evaporation of most of the water present in black liquor. During devolatilization the organic compounds in black liquor solids are thermally degraded to yield combustible gases and residual char. This char is a black, porous, and friable material consisting primarily of organic carbon and the inorganic salts Na_2CO_3, Na_2SO_4, and Na_2S. Approximately one-half of the carbon and most of the sodium contained in the incoming black liquor are found in the char [3]. On a molar basis, carbon is the dominant species and excess reactant in the char.

Char burning consists of heterogeneous reactions that can occur either in-flight or on the char bed in which the residual carbon is oxidized to CO and CO_2. During char burning, the primary oxidizer is O_2 in the combustion air. The O_2 depletes the carbon in the char through direct oxidation and through the sulfate/sulfide cycle [1,4]. Blackwell and King [5] have reported O_2 concentrations from 2 to 4% immediately above the bed, and from 14-18% at a height of 20 to 30 inches above the bed. The low O_2 concentrations next to the char bed suggest that other oxidizer species such as CO_2 and H_2O may play an important role in carbon oxidation. This is supported by results from a recent effort in three-dimensional mathematical modeling of the kraft recovery furnace by Grace et al. [6]. Addition of the CO_2 and H_2O gasification reactions to the char bed portion of the model altered the predicted result from one in which there was substantial buildup of carbon on the bed to one where the carbon burning rate was approximately equivalent to the rate of carbon reaching the bed.

PREVIOUS CO_2 GASIFICATION RATE STUDIES

Li and van Heiningen [7,8] used a thermogravimetric analysis system to study the CO_2 gasification rate of small quantities (~5 mg) of slow and fast pyrolysis black liquor chars (BLC) between 600°C and 800°C. The fast pyrolysis char was made by pyrolyzing black liquor solids for 20 minutes under N_2 with 10% CO in a tube furnace pre heated to 580°C. The slow pyrolysis char was prepared by raising the temperature from 20°C to 775°C at a rate of 25 degrees per minute. The reported gasification rate of BLC was 10-20 times greater than that obtained for activated carbon or coal chars impregnated with Na_2CO_3. It was shown that the high loading and fine distribution of sodium in BLC were responsible for the high gasification rates. The rate of BLC gasification was also influenced by the method of black liquor drying because drying influenced the sodium dispersion. The influences of gas composition on BLC gasification were modeled using Langmuir-Hinshelwood type kinetics; activation energies (44.7 kcal/mol for slow pyrolysis char, 60.0 kcal/mol for fast pyrolysis char) were similar to activation energies for burning alkali metal impregnated porous carbon. The CO inhibition was relatively small, and the gasification rate was first-order in carbon up to 80% conversion. Internal surface area of BLC appeared to have an influence on the gasification rate.

Frederick and Hupa [9,10] studied the kinetics of CO_2 gasification of small quantities of BLC (~100mg) at similar temperatures but using a pressurized thermobalance system to produce pressures between 1 and 30 bars. The rate of gasification was found to be slightly less than first-order in CO_2 and strongly inhibited by CO at higher pressures. At constant gas composition and temperature, the rates of gasification of BLC with CO_2 were slowed as pressure was increased. Frederick and Hupa [9,10] reported an activation energy of 44.4 kcal/mol for the CO_2 gasification reaction. The rate varied by a factor of two at identical gasification conditions for experiments with chars from three different liquors.

Goerg and Cameron [11,12] studied the CO_2 gasification of a kraft char and Na_2CO_3 mixture using a fixed bed purge reactor. Goerg and Cameron suggested that the inhibiting effect of CO caused

the rate of reaction to be less than first-order in carbon concentration. A Langmuir-Hinshelwood model of the gasification reaction agreed closely with the experimental results. From the experimental results, the following were concluded by Goerg and Cameron: as the CO concentration increases, the rate decreases; as the CO_2 concentration increases, the rate levels off; and as the CO and CO_2 concentration are lowered, the rate is proportional to the CO_2 concentration. Based on the high activation energy (46.8 kcal/mol) and experimental results, Goerg and Cameron concluded that the CO_2 gasification reaction is kinetically controlled rather than mass transfer controlled for the range of experimental temperatures (1200-1283K) tested.

The rates from Goerg and Cameron [11,12] were much slower than the rates reported by Li and van Heiningen [7,8] and Frederick and Hupa [9,10]. However, the activation energies reported by each group of investigators were in agreement.

The studies of Li and van Heiningen [7,8] and Frederick and Hupa [9,10] employed BLC gasification using small quantities of char and thermogravimetic analysis. Goerg and Cameron [11,12] used a Kraft char and Na_2CO_3 mixture and fixed bed purge reactor. A primary objective of this study was to provide independent CO_2 gasification rate data using larger quantities of BLC in a fixed bed reactor. An additional goal was to apply the results of this work toward a better understanding of the rate controlling processes for CO_2 gasification in recovery furnaces.

EXPERIMENTAL PROCEDURE

Rate data were obtained with BLC made from black liquor received from a Southeastern U.S. kraft mill pulping a mixture of hardwood and softwood. Partially pyrolyzed char particles were formed by injecting single black liquor droplets downward into upward flowing air using a drop tube furnace as described by Clay et al. [13]. The drop tube furnace temperature was approximately 950°C; the initial black liquor droplet diameter was 2 mm; the particle retention time was approximately 2 second;, and the mean char particle diameter was 7.7 mm. The partially pyrolyzed particles were fully pyrolyzed by further heating in a cylindrical fixed bed reactor (7.1 cm diameter by 15.2 cm depth), shown in Fig. 1. This was accomplished at atmospheric pressure with a mixture of 95%N_2/5%CO flowing through the fixed bed at a flow rate of approximately 5 slpm. Li [15] suggests that Na_2CO_3 will react with organic carbon yielding products such as gaseous Na, CO, and some CO_2. Therefore, CO was included in the preheat gas to prevent the Na_2CO_3-Char C reaction. The CO and CO_2 concentrations in the product gases were measured continuously using an infrared analyzer. Pyrolysis was considered to be complete when the CO and CO_2 concentrations in the product gas approached 5% and 0% (the levels of CO and CO_2 in the feed).

The elemental compositions of the resulting chars, shown in Table I, were significantly affected by the pyrolysis temperature used in the fixed bed. For the gasification experiments in this study, the pyrolysis temperature (and, hence, the char composition) was chosen to be the same as the gasification temperature. This choice of pyrolysis temperature was made primarily for convenience, as gasification of the char was initiated immediately upon completion of pyrolysis.

Gasification was initiated by replacing the CO in the carrier gas with the desired level of CO_2. The product gases were monitored continuously for CO and CO_2 concentrations. Table II contains the ranges of conditions used in the gasification experiments. The reason for using different carrier gas and carrier gas flow rates was to quantify mass transfer effects on the observed rate.

DATA ANALYSIS AND DISCUSSION

A typical set of CO and CO_2 concentration profiles obtained is shown in Fig. 2. The rate of gasification was determined from the CO_2 concentration profiles according to a method outlined by Smith [14] for a fixed bed in which the solid particles contain one reactant, and the second reactant is in the fluid phase. The CO_2 concentration decreased along the reactor length, and this variation of concentration with length was a function of time. Thus, the process did not operate at steady state. For isothermal plug-flow, a mass conservation equation for CO_2 is written as:

$$-u\frac{\partial(C_{CO2})}{\partial z} = r\rho_{bed} + \varepsilon_{bed}\frac{\partial(C_{CO2})}{\partial t} \qquad (1)$$

where ρ_{bed} = density of char bed, (kg organic C/m^3)
$r\rho_{bed}$ = global rate of disappearance of CO_2 per unit volume of reactor, (gmole/m^3/s)
u = superficial velocity in the direction of flow, (m/s)
ε_{bed} = void fraction of char bed
z = axial position in the char bed, m
t = time, s

Over small increments of time (1 to 2 min in Fig. 2), the CO_2 concentration is approximately constant, and the time derivative in Eq. 1 can be considered negligible. Assuming a first-order global rate for CO_2 gasification of BLC (i.e., $r = k[C_{CO2}]$), Eq. 1 can be integrated and rearranged to solve for the rate constant,

$$k = \frac{u}{L\rho_{bed}} \ln\frac{(C_{CO2})_{feed}}{(C_{CO2})_{exit}} = \frac{uA}{m} \ln\frac{(C_{CO2})_{feed}}{(C_{CO2})_{exit}} \qquad (2)$$

where A = total cross-sectional area of the fixed bed reactor
m = mass of organic carbon in the fixed bed reactor
L = char bed height

Evaluation of Eq. 2 at Δt increments of one minute yields the rate constant as a function of fractional conversion of organic carbon. Fig. 3 shows the results for experimental data shown in Fig. 2.

The high rate constant at fractional conversion less than 0.1 is a result of lag from the time CO_2 is added to the time the IR analyzer detects the product gas concentration. Values for average rate constant were determined from the data in Fig. 3 for conversions greater than 0.1. Fig. 3 shows that the rate constant is independent of fractional conversion of organic carbon, thereby, verifying the assumption that the reaction is first order with respect to CO_2.

An Arrhenius plot for the 600°C, 700°C, and 800°C data is shown in Fig. 4. The low rate constant values at 800°C seem to indicate the presence of mass transfer limitations at this temperature. However, tests were performed to evaluate mass transfer effects and showed the observed rate was not limited by mass transfer. To test for film mass transfer effects, experiments were performed using different gas velocities. Experiments were completed using He as the carrier gas and compared to the results where N_2 was the carrier gas to test for pore diffusion effects. As shown in Table III, the resulting average rate constants were approximately the same indicating that neither film nor pore diffusion effects were appreciable. In addition, the average film mass transfer coefficient was calculated using a correlation for packed beds as [14]

$$k_m a_m = \left(\frac{0.455}{\varepsilon_{bed}}\right)\left(\frac{u d_p \rho}{\mu}\right)^{-0.407}\left(\frac{\mu}{\rho D_{AB}}\right)^{-2/3} a_m u \qquad (3)$$

where a_m = external surface area per unit mass
d_p = average diameter of the char particles
μ = viscosity of the fluid
ρ = density of the fluid
D_{AB} = molecular diffusivity of component being transferred

The other quantities are as defined for Eq. 1. The average film mass transfer coefficient predicted at 800°C was 7.1 $m^3/kg/s$, which is more than an order of magnitude greater than the observed rate constant. Consequently, film mass transfer and pore diffusion limitations in the fixed bed reactor were considered negligible at 800°C.

Oxygen material balances show that take-up of oxygen by the char bed is an explanation for the lower than expected rate constants at 800°C. Assuming that the only reaction occurring was Char-C + CO_2--->2CO, the mass flow rate of oxygen entering in CO_2 should equal the mass flow rate of oxygen leaving in CO and CO_2. The ratio of oxygen out to oxygen in at 600°C and 700°C was very close to unity (0.98± 0.03), while the average ratio for 800°C experiments was significantly less than unity (0.85± 0.02). This suggests that oxygen was consumed by competing reactions during the high temperature experiments.

Two observations, the formation of smelt and corrosion of the reactor walls, support oxygen consumption as an explanation for the lower than expected rate constants obtained at 800°C. First, two distinct residual solids were observed following each 800°C experiment. One solid was similar to the friable starting material, whereas the other solid was beads of frozen smelt that were attached to nearby stainless steel. In the 800°C experiments, the fractional conversion of organic carbon ranged from 70%-99% depending on experimental conditions such as CO_2 concentration and gas flow rate. Grace et al. [3] have noted that as the organic carbon in char is decreased, the inorganics in the char will coalesce to form smelt. As the organic carbon is depleted, the oxidizer (CO_2) will react with the inorganics. For example, the Na_2S in the char would react with CO_2 to form Na_2SO_4 ($Na_2S + 4CO_2 <---> Na_2SO_4 + 4CO$). Elemental analysis allowed the sulphur concentration of the initial char and residual friable char to be determined. By assuming that no sulphur was vaporized and the remaining sulfur would exist as Na_2SO_4 in the frozen smelt, material balances showed (see Table IV) that 64-76% of the unaccountable oxygen was used to produce this Na_2SO_4.

The second observation, corrosion of the stainless steel reactor walls, was observed by weight loss of the reactor walls during the 800°C experiments. Before and after each experiment, the reactor tube that held the char was weighed to determine the weight loss encountered during each experiment. In addition, the reactor tube was cleaned following each experiment to remove the corrosion scale from

the reactor walls. Assuming that the weight loss was primarily Cr_2O_3, it was determined as shown in Table IV that 13-43% of the unaccountable oxygen appeared in the Cr_2O_3.

Thus, smelt reactions and corrosion reactions accounted for all (95-107%) of the discrepancies in oxygen material balances for the 800°C tests and are likely responsible for the lower than expected rate constant values by consuming part of the CO_2. The activation energy for 600°C, 700°C, and 800°C data is 41,200 cal/mol. However, the activation energy for 600°C and 700°C data, 48,900 cal/mol, is a more appropriate value, since the interfering reactions at 800°C lower the rate constants at this temperature.

Comparison to Previously Reported Results

Table V summarizes the rates, activation energies, and conditions of the available BLC gasification experiments. Considering that different chars will yield somewhat different rates, there is fair agreement in rates among the various investigations excepting the Goerg and Cameron data. Goerg and Cameron [11,12] used a mixture of char and Na_2CO_3 as the starting material, whereas char was the only solid reactant used in other studies. Goerg and Cameron [11,12] heated the char-Na_2CO_3 mixture to reaction temperature in an atmosphere of N_2 gas. As char-Na_2CO_3 mixture is heated to reaction temperature, Li [15] suggests that Na_2CO_3 will react with organic carbon yielding products such as gaseous Na, CO, and some CO_2. Therefore, it is likely that the initial organic carbon concentration for the Goerg and Cameron experiments was low if not negligible. Since the rate of gasification is a function of the organic carbon concentration, low organic concentration at the beginning of gasification would have resulted in much slower observed gasification rates than the observed rates of the other studies. In addition, the inherent kinetic rate was probably not measured since the CO_2 never reached the surface of the char because of poor mixing which resulted from the low concentration of char in the smelt.

The rates of this study are somewhat faster than the rates reported in the other studies when the differences in CO_2 concentrations are considered. The CO_2 concentration of this study (4.4%) was lower than the CO_2 concentration of Frederick and Hupa [9,10] and Li and van Heiningen [7,8] (20%). For example, if 20% CO_2 had been used in this study, the projected rate would be 7.5 hr^{-1} which is approximately 1.6-8.3 times faster than the rates reported by others. The activation energy of this study compares well to the activation energies reported by others. The similarities in rates and activation energies are significant considering the differences in char quantity, liquors used to produce the chars, the char production process, and the differences in the experimental reactors.

IMPLICATIONS FOR KRAFT RECOVERY FURNACES

Having established a rate constant for the gasification of black liquor char by CO_2, the implication of these results for kraft recovery furnaces were examined. Brown et al. [16] measured mass transfer coefficients for the burning rates of black liquor char in O_2 and developed the following empirical correlation.

$$k_m = 2.78 \cdot u^{0.91} \tag{4}$$

where k_m = mass transfer coefficient (cm/s)
u = velocity of gas (m/s)

Eq. 4 can be applied to predict mass transfer rates for CO_2 by accounting for differences in gas density and diffusivity according to the dependencies shown in Eq. 3. This results in reducing the constant in Eq. 4 to 2.57 for mass transfer for CO_2. Eq. 4 is applied using the typical furnace conditions in Table VI. Using these typical conditions, the primary air velocity is determined as

$$u = [A \cdot B \cdot C \cdot D \cdot E]/[F \cdot G] = 7.59 m/s \tag{5}$$

The external surface area per unit mass is determined as

$$a_m = B/[B \cdot H \cdot I] = 2.57 m^2/kgC \tag{6}$$

Substitution of the calculated primary air velocity into Eq. 4 results in a mass transfer coefficient of 0.15 m/s. Multiplication of the external surface area per unit mass by this mass transfer coefficient yields a value that can be compared to the global rate constant as

$$k_m a_m = 0.15(m/s) \cdot 2.57(m^2/kgC) = 0.39(m^3/kgC/s)$$

Referring to Fig. 4, it is seen that the measured rate of CO_2 gasification takes on this value at approximately 765°C. In other words, the temperature where the rate of CO_2 mass transfer is equivalent to the kinetic rate of CO_2 gasification is approximately 770°C. At higher temperatures, the burning rate will be controlled primarily by the rate of mass transfer of CO_2.

Table VII summarizes the range of recovery boiler parameters which influences the mass transfer and kinetic rates of BLC gasification, as well as the mass transfer coefficient (calculated from Eq. 4) and kinetic rate constants (from the data in Fig. 4) based on these parameters. As expected, higher temperatures, slower gas velocities, and larger active char layers promote mass transfer control of the CO_2 gasification reaction. For typical recovery furnace parameters where the bed temperature is 1250 K, gas velocity is 10 m/s, and the active char layer is 6 cm; the rate of CO_2 gasification is clearly mass transfer controlled. In general, within the range of parameters in TableVII, the kinetic coefficient is always much greater than the mass transfer coefficient leading to the conclusion that CO_2 gasification rate in a recovery furnace is typically mass transfer controlled.

SUMMARY & CONCLUSIONS

The CO_2 gasification rate of kraft black liquor char was studied using a fixed bed reactor at temperatures of 600°C, 700°C, and 800°C. Experiments using different gas velocities and different carrier gases (N_2 or He) showed that the observed rate was not affected by film mass transfer or pore diffusion. The rate of CO_2 gasification and the activation energy (E_A=48kcal/mol) derived from the data compare well to rates and activation energies reported for previous thermogravimetric investigations. These similarities in rates and activation energies are significant considering the differences in char quantity, liquors used to produce the chars, the char production processes, and the experimental reactors.

The values determined for gasification rate constant at 800°C were somewhat lower than expected. This was shown by material balances on oxygen to be due to other CO_2 consuming reactions, namely smelt oxidation and corrosion.

Using the measured CO_2 gasification rates, the implications for kraft recovery furnaces were examined. Application of the CO_2 gasification rate to typical recovery furnace operating conditions shows that CO_2 gasification becomes mass transfer controlled at approximately 800°C. Since most of the lower furnace volume is expected to be at temperatures greater than 800°C, the rate of CO_2 gasification in recovery furnaces is expected to be mass transfer limited rather than kinetically controlled. Caution should be used, however, in applying these results in a predictive recovery furnace model where oxygen combustion and CO_2/H_2O gasification are occurring simultaneously. These various carbon consuming reactions may not be occurring strictly in parallel but rather there may be significant reaction blocking occurring. This blocking should be the subject for further study in both CO_2 and H_2O gasification.

LITERATURE CITED

1. GRACE, T.M.; CAMERON, J.H.; and CLAY, D.T, "Role of the Sulfate-Sulfide Cycle in Char Burning: Experimental Results and Implications", TAPPI 69(10): 108-113 (1986).

2. ADAMS, T.N. and FREDERICK, W.J, Kraft Recovery Boiler-Physical and Chemical Process, The American Paper Institute (1988).

3. GRACE, T.M.; CAMERON, J.H.; and CLAY, D.T., Char-Burning Project 3473-6, The American Paper Institute (February 22, 1985).

4. CAMERON, J.H. and GRACE, T.M. "Kinetic Study of Sulfate Reduction with Carbon", Ind. Eng. Chem. Fundam. 22(4): 486-494 (1983).

5. BLACKWELL, B. and KING, T. Chemical Reactions in Kraft Recovery Boilers, Vancouver: Sandwell and Company Limited, (1985).

6. GRACE, T.M.; WALSH, A.; JONES, A.; SUMNICHT, D.; and FARRINGTON, T., "A Three-Dimensional Mathematical Model of the Kraft Recovery Furnace", Proc. 1989 Intl. Chem. Recovery Conf., Ottawa, April 3-6, 1989, p. 1-8.

7. LI, J. and VAN HEININGEN, A.R.P., "Reaction Kinetics of Gasification of Black Liquor Char", The Can. J. of Chem. Eng. 67(8): 693-697 (1989).

8. LI, J. and VAN HEININGEN, A.R.P., "Kinetics of CO_2 Gasification of Fast Pyrolysis Black Liquor Char", Ind. Eng. Chem. Res. 29(9): 1776-1785 (1990).

9. FREDERICK, W.J. and HUPA, M., "Gasification of Black Liquor Char with CO_2 at Elevated Pressures. TAPPI 74(7): 177-184 (1991).

10. FREDERICK, W.J. and HUPA, M., "Gasification of Black Liquor at Elevated Pressures Part 2. Rate Data with CO_2 and Water Vapor", Combustion Chemistry Research Group Report 90-12, Abo Akademi, Turku, Finland (1990).

11. GOERG, K.A. and CAMERON, J.H., "A Kinetic Study of Kraft Char Gasification with CO_2", AICHE Meeting, Boston, Preprint no. 67g: (Aug. 24-27, 1986).

12. GOERG, K.A. The Gasification of Kraft Char with Carbon Dioxide, M.S. Dissertation, Appleton, WI, The Institute of Paper Chemistry, (1986).

13. CLAY, D.T.; GRACE, T.M.; KAPHEIM, R.J.; SEMERJIAN, H.G.; MACEK, A.; and CHARAGUNDLA, S.R., "Fundamental Studies of Black Liquor Combustion", Report No. 1-Phase 1, U.S. DOE Report No. DE85013773 (January 1985).

14. SMITH, J.M., Chemical Engineering Kinetics, New York: McGraw-Hill Book Company, pp. 394-397 and 655-658 (1981).

15. LI, J., Pyrolysis and CO_2 Gasification of Black Liquor Char, M. Eng. Thesis, Montreal, McGill Univ., (February 1986).

16. BROWN, C.A.; GRACE, T.M.; and CLAY, D.T., "Char Bed Burning Rates-Experimental Results", Proc. 1989 Intl. Chem. Recovery Conf., Ottawa, April 3-6, 1989, pp. 65-73.

17. MCCANN, D., "A review of Recovery Boilers Process Design", 77th Annual Meeting Technical Section Canadian Pulp & Paper Association: A49-A58 (Jan. 29-30, 1991).

18. HOUGH, G., Chemical Recovery in the Alkaline Pulping Process, Atlanta: p. 148, TAPPI Press (1985).

Portions of this work were used by Stacy R. Lee as partial fulfillment of the requirements for the Ph.D. degree at the Institute of Paper Science and Technology.

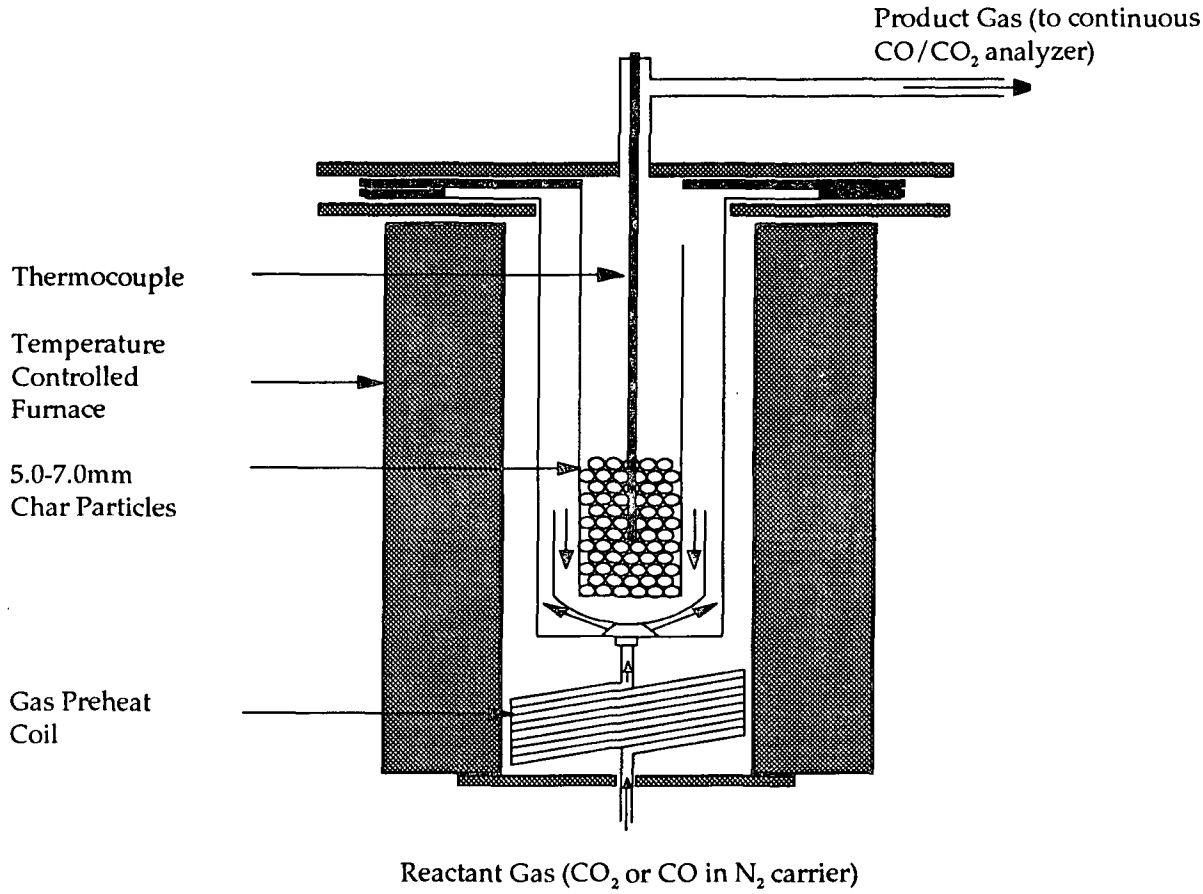

FIGURE 1: Schematic for Fixed Bed Reactor Used for CO_2 Gasification of Black Liquor Char

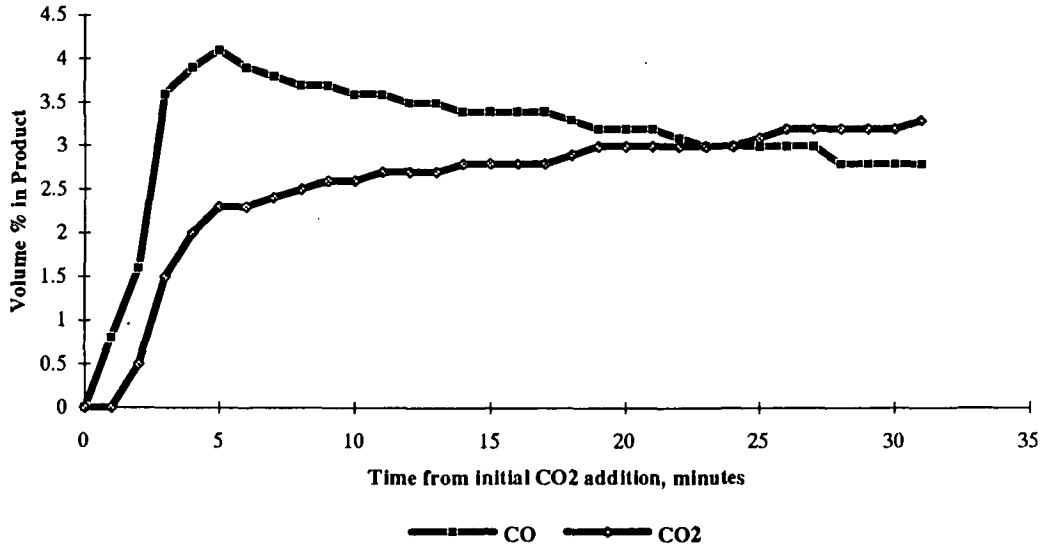

FIGURE 2: %CO and %CO_2 in Product Gas as a Function of Time for a Typical Gasification Experiment (702°C, 4.3% CO_2, 5.3 slpm, N_2 Carrier Gas)

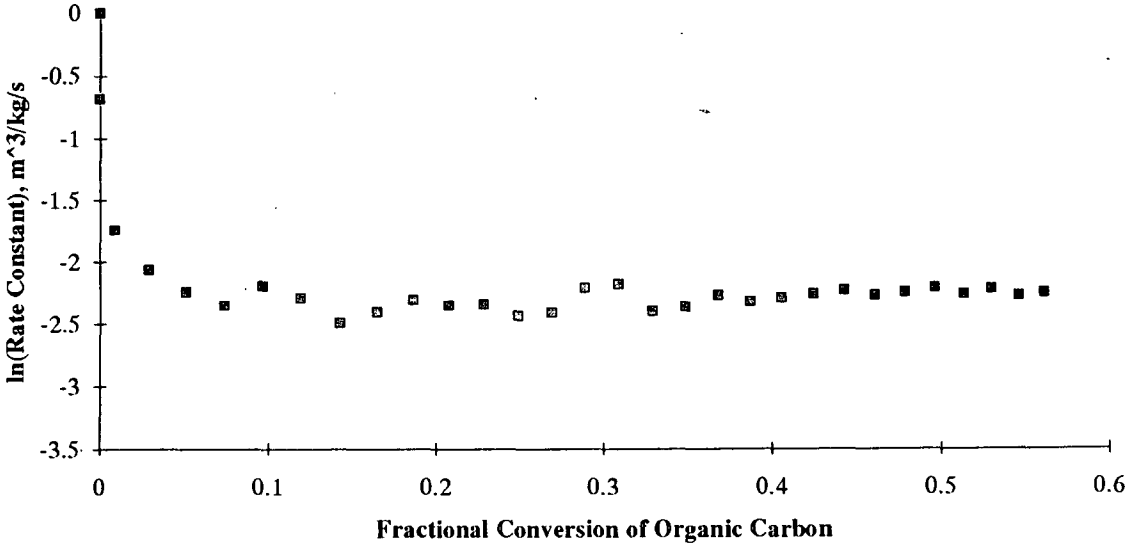

FIGURE 3: Rate Constant vs. Fractional Burnout of Organic Carbon for a Typical Gasification Experiment (702°C, 4.3% CO_2, 5.3 slpm, N_2 Carrier Gas)

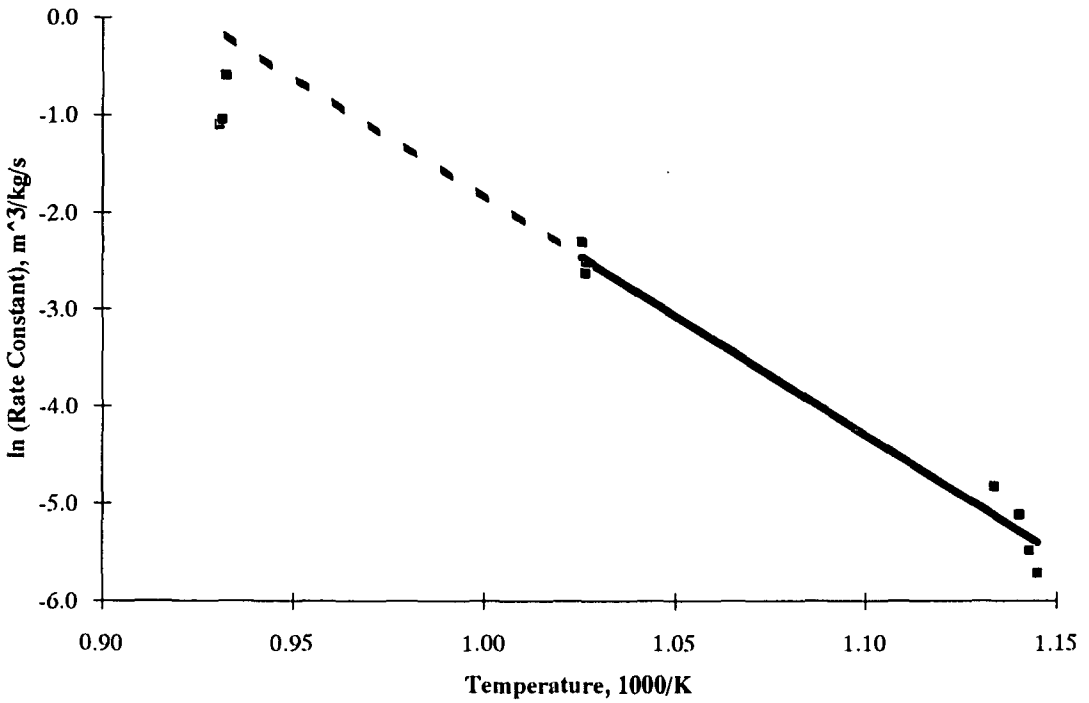

FIGURE 4: Arrhenius Plot for Data at 600°C, 700°C, and 800°C

Table I: Composition (Weight %) of BLC used in Fixed Bed Reactor Experiments

	Pyrolysis Temperature		
Element	600°C	700°C	800°C
C	34.1	28.2	25.3
H	1.35	0.86	0.48
O	30.5	28.6	31.8
Na	25.2	27.4	26.1
S	3.75	4.23	5.54
Carbonate C	5.11	6.63	6.62
Sulfate S	1.74	1.32	2.21
Thiosulfate	0.22	0.63	0.22

Table II: Ranges of Conditions in the Fixed Bed Reactor Experiments

Parameter	Value
Temperature	600°C, 700°C, 800°C
Pressure	1 atmosphere
CO_2 Concentration	4.3%-10.1%
Carrier Gases	He, N_2
Gas Flow Rate	5.32 slpm, 10.10 slpm
Char Mass	10-15 g

Table III: Comparison of Rate Constants for Varying Mass Transfer Conditions

Carrier Gas	Superficial Gas Velocity, m/s	Rate Constant, $m^3/kg/s$	Calculated M.T. Coeff., $m^3/kg/s$
N_2	0.08	0.47(+/-)0.20	7.07
He	0.08	0.53(+/-)0.17	10.6
N_2	0.17	0.30(+/-)0.14	10.6

Table IV: Oxygen Consumed by Competing Reactions

Experiment Number	mgmole O_2 Unaccounted for	mgmole SO_4 in Smelt	mgmole Cr_2O_3 in Corrosion Products	% of Unaccountable O_2 to form Sulphate	% of Unaccountable O_2 to Corrosion
4,905	93.7	17.8	5.92	76	19
4,906	164	16.8	7.24	NA	13
4,907	116	18.7	16.4	64	43

Table V: Comparison of CO_2 Gasification Rates

Rate @ 700°C (hr^{-1})	E_A (kcal/mol)	Temp. Range (°C)	Gas Pressure. (atm.)	Gas Composition, % $CO_2/CO/N_2$	Exp. Method	Char Mass, (g)	Investigator
1.9	44.4	700-900	1	20/4/76	PTG*	~0.1	Frederick& Hupa [9]
0.9	49	650-800	20	20/4/76	PTG	~0.1	Frederick & Hupa [10]
3.0-4.8	60	675-775	1	20/10/70	TGA**	~0.005	Li & van Heiningen [8]
1.1	44.7	700-775	1	20/10/70	TGA	~0.005	Li & van Heiningen [7]
2.52E-3	46.8	927-1010	1	5/5/90	Purged Bed	1	Goerg & Cameron [11,12]
1.7	48.9	600-800	1	4.4/0/95.6	Fixed Bed	10-15	Present Study

*PTG=Pressurized Thermogravimetric

**TGA=Thermogravimetric Analysis

Table VI: Typical Furnace Conditions Used in the Application of Derived CO_2 Rate to Recovery Furnaces

Parameter	Assumed Value	Variable
Hearth Loading [17]	0.21 kg/sm^2	A
Boiler Cross-sectional Area [2]	100 m^2 (10mx10m)	B
Air Requirement	6 kg Air/kg Black Liquor Solids	C
Primary Air Distribution [18]	45% of Total Air Requirement	D
Primary Air Into One Wall	25% of Total Primary Air	E
Channel of Air Flow	6.67 m^2 (10mx667m)	F
Density of Air	0.28 kg/m^3	G
Density of Char	7.79 kgC/m^3	H
Acitve Burning Layer [16]	5 cm	I

Table VII: The Influence of Recovery Furnace Parameters on Mass Transfer and Kinetic Rate Constants

Parameter	Low	Typical	High
Temperature (K/°F)	1030/1400	1250/1800	1480/2200
Velocity Range (m/s)	0.5	10	65
Active Char Layer (cm)	3	6	10
Kinetic Coeff. (m^3/kgC/s)	0.2	13.6	290
Mass Transfer Coeff. (m^3/kgC/s)	0.05	0.2	1.39